Current Research in Food Science 5 (2022) 1–10

Contents lists available at ScienceDirect

Current Research in Food Science

journal homepage: www.sciencedirect.com/journal/current-research-in-food-science

Analyzing the phenolic enriched fractions from Nixtamalization wastewater (Nejayote) fractionated in a three-step membrane process

Elsa Díaz-Montes [a,**], Roberto Castro-Muñoz [b,c,*]

[a] Unidad Profesional Interdisciplinaria de Biotecnología, Instituto Politécnico Nacional, Av. Acueducto s/n, Barrio La Laguna Ticoman, Ciudad de México, 07340, Mexico

[b] Gdansk University of Technology, Faculty of Chemistry, Department of Process Engineering and Chemical Technology, 11/12 Narutowicza St., 80-233, Gdansk, Poland

[c] Tecnologico de Monterrey, Campus Toluca. Av. Eduardo Monroy Cárdenas 2000, San Antonio Buenavista, Toluca de Lerdo, 50110, Mexico

ARTICLE INFO

Keywords:
Nixtamalization
Nejayote
Membrane processes
Carbohydrates
Sugars
Phenolic fractions

ABSTRACT

Nejayote is recognized as the main by-product resulting from the nixtamalization process of maize kernels, which is categorized as an alkaline residue with a chemical composition based on carbohydrates (37.8–55.7%), fiber (22.8–25.5%), protein (4.9–7.4%), and lipids (0.4–1.5%). In addition, Nejayote has an extensive content of simple (e.g., phenolic acids) and complex phenolic compounds (e.g., anthocyanins), which are responsible for the pigmentation and antioxidant activity of maize; therefore, there is a need of their identification depending on the type of maize. The current research has focused on the efficient extraction and identification of the phenolic acids contained in Nejayote after the processing of different types of maize. The target of this work was to fractionate Nejayote from white (NWM), red (NRM), and purple maize (NPM), using three different membranes, such as microfiltration (MF with a pore size of 1 μm) and ultrafiltration (UF100 and UF1 with a molecular weight cut-off of 100 kDa and 1 kDa, respectively), which were strategically applied to extract phenolic acids while retaining other molecules. Such a membrane system exhibited a retention in the first stage of almost all carbohydrates (MF-Retentate: ca. 12–19 g GE/L), while second stage (UF100-Permeate) a concentration of phenolic components was recovered ranging from 768 to 800 mg GAE/L. Finally, in the third stage (UF1-Permeate), 14 phenolic acids were identified, including ferulic and *p*-coumaric acids, derived from caffeic and ferulic acids, along with other molecules (e.g., glucose and fructose).

1. Introduction

Nixtamalization is a thermal-alkaline protocol applied to maize that allows the partial or total elimination of the pericarp from the kernel; this protocol generates two main products the so-called nixtamal and Nejayote. Nixtamal represents the softened grains that serve as ingredients for the preparation of tortillas, flour, and other nixtamalized maize products; while Nejayote is the alkaline wastewater resulting from cooking kernels (Serna-Saldivar and Rooney, 2015). This by-product is generated in large volumes due to the demand for nixtamal since nixtamalized products are the first necessity foods in Latin America. A traditional nixtamalization process requires up to 7.5 L of water per kg of maize, which becomes Nejayote (Díaz-Montes et al., 2018).

There is evidence suggesting that the Nejayote can be reused as cooking water in following nixtamalization process, which would help to save clean water and reduce its production (Valderrama-Bravo et al., 2015). On the other hand, several treatments have been implemented to reduce the organic load from Nejayote, for example, the use of laccases, activated sludge, or biological reactors to reduce the organic solids and COD (Díaz-Montes et al., 2016, 2018). Other investigations have focused on utilizing Nejayote as culture media (for *Aspergillus awamori*, *Paenibacillus amylolyticus*, *Pseudomonas putida and Acinetobacter*), animal feed (for broilers) (Velasco-Martinez et al., 1997) or in bakery products (Díaz-Montes et al., 2016), considering that Nejayote has a high carbohydrate content (between 37.8 and 55.7%, dry base), crude fiber (between 22.8 and 25.5%, dry base), protein (between 4.9 and 7.4%, dry base), crude fat (between 0.4 and 1.5%, dry basis) and ash (between

* Corresponding author. Gdansk University of Technology, Faculty of Chemistry, Department of Process Engineering and Chemical Technology, 11/12 Narutowicza St., 80-233, Gdansk, Poland.

** Corresponding author.

E-mail addresses: elsadimo123@gmail.com (E. Díaz-Montes), food.biotechnology88@gmail.com, castromr@tec.mx (R. Castro-Muñoz).

https://doi.org/10.1016/j.crfs.2021.11.012

Received 13 September 2021; Received in revised form 9 November 2021; Accepted 22 November 2021

Available online 25 November 2021

12.7 and 33.6%, dry basis) (Velasco-Martinez et al., 1997). Additionally, Nejayote has also been appreciated as a source to obtain specific phenolic compounds (e.g., ferulic and *p*-coumaric acids) (Gutiérrez-Uribe et al., 2010; Niño-Medina et al., 2009); which depend on the type of corn they come from, for example, pigmented corn is composed of large amounts of anthocyanins (Bello-Pérez et al., 2016), carotenoids (Bacchetti et al., 2013), and phenols (Hernández-Martínez et al., 2016), while phenolic acids predominate in white corn (Syedd-León et al., 2020).

Phenolic components are secondary metabolites that originate from primary metabolites (e.g., carbohydrates, amino acids, and lipids) in plant species as a means of protection against pests (i.e., insects, viruses, and bacteria) and UV radiation (Kumar and Goel, 2019). These components can be grouped into simple phenols (e.g., phenolic acids and polyphenols) and complexes (e.g., tannins, lignins, and flavonoids), which are associated with the color and properties of each plant species (Kumar and Goel, 2019; Méndez-Lagunas et al., 2020). Within the diet, phenolic components are considered as active ingredients due to their biological activity including antioxidant, anti-inflammatory, antimicrobial, anti-cancer, and anti-allergenic activity; and they related to the prevention and treatment of chronic and acute diseases (e.g., heart diseases, immune disorders, and cancer) of the human being (Galanakis et al., 2020). In addition, the bioactive activity is associated with the induction of enzymes, inhibition of reactions and protection against external pathogens (Galanakis, 2021), because they strengthen the immune system (Galanakis, 2020; Galanakis et al., 2021).

The recovery of phenolic components from plant sources is carried out through the *5-Stage Universal Recovery Process*, which consists of pretreatment, molecule separation, extraction, purification and obtaining products (Galanakis, 2012). The extraction stage in a conventional way includes the use of organic solvents (e.g., acetone, ethanol, chloroform, and methanol) (Díaz-Montes et al., 2021; Díaz-Montes and Castro-Muñoz, 2019; Nagarajan et al., 2016) or hydrotropic solvents (e.g., nicotinamide, sodium cumene sulfonate, sodium salicylate, resorcinol, and citric acid) (Nagarajan et al., 2016). In recent decades, alternative technologies have been implemented that include accelerated solvent extraction, ultrasonication-assisted extraction, high-voltage electrical discharges, microwave-assisted extraction, pulsed electric fields, and ultrasound-assisted extraction (Bursać Kovačević et al., 2018; Deng et al., 2015; Díaz-Montes et al., 2021). Conventional technologies fulfill the purpose of extracting components from plant sources in a shorter time and controlled temperature (Sarfarazi et al., 2020); however, most of them need large amounts of inputs, have high production costs, and generate low process performance (Galanakis et al., 2016). In this way, membrane-based technologies have been implemented in the recovery of high added-value components (e.g., proteins, fibers, sugars, and phenolic compounds) (Galanakis, 2015) from different systems, such as plant sources (Arboleda Mejia et al., 2020; Conidi et al., 2020; Díaz-Montes et al., 2020a), fermentation broths (Díaz-Montes et al., 2020b; Díaz-Montes and Castro-Muñoz, 2019; Prochaska et al., 2018), and agro-industrial waste by-products (Castro-Muñoz et al., 2021; Chen et al., 2019; Díaz-Montes et al., 2018).

The aim of this work was the fractionation of Nejayote via three-step membrane process including microfiltration (MF) and ultrafiltration (UF) membranes. Such a process allowed us to recover carbohydrates, sugars, and phenolic compounds coming from white (NWM), red (NRM), and purple maize (NPM). Then, the latter fraction was extensively analyzed identifying the phenolic acids and polyphenols present in Nejayote.

2. Materials and methods

2.1. Preparation of Nejayote

Three varieties of maize kernels (*Zea mays*) were used: Mushito from Michoacán (white), Elote Occidental (red) and Elotero from Sinaloa (purple); which were obtained in a local market in Pátzcuaro, Michoacán, Mexico. The wastewater was generated through a traditional nixtamalization process, in which the maize was heated (90 °C, 40 min) in alkaline calcium hydroxide solution (0.33%, w/v) in 1:3 ratio (w/v). The kernels were left to stand in the alkaline solution for 16 h and were subsequently drained. The kernels were then washed twice (3.5 L each time), and the drained wastewater was allowed to sediment (25 °C, 5 h). This process was repeated to obtain Nejayote from white (NWM), red (NRM), and purple maize (NPM).

2.2. Experimental set-up and procedures for the fractionation of Nejayote

The fractionation of Nejayote consisted in smartly applying a sequential membrane process involving a MF membrane and two UF membranes with different molecular weight cut-off (MWCO). The main specifications of such membranes are detailed in Table 1.

As part of the characterization of the process, the permeate flux (J_p, L/m^2 h) was determined as the permeate volume per unit area and time (at 25 °C, feed flow rate (Q_f) of 58 L/h), as represented in Eq. (1):

$$J_p = \frac{V_p}{A * t} \tag{1}$$

where V_p (expressed in L) corresponds to permeate volume, A (m^2) corresponds to the membrane area, and t (h) corresponds to the operating time (Díaz-Montes et al., 2020a). The volume reduction factor (VRF), as denoted by Eq. (2), expresses the ratio between feed (V_F, expressed in L) and retentate (V_R, L) volumes (Díaz-Montes et al., 2020a):

$$VRF = \frac{V_F}{V_R} \tag{2}$$

A common parameter that dictates the selectivity of a membrane in pressure-driven membrane processes is the rejection (R, %), which was calculated using Eq. (3):

$$R_i = \left(1 - \frac{C_{Pi}}{C_{Fi}}\right) * 100 \tag{3}$$

where C_F (g/L) and C_P (g/L) correspond to the concentration of specific compound (*i*) in feed and permeate streams, respectively. The limiting transmembrane pressures (TMP_{lim}) for MF, UF100 and UF1 steps were as 1.3, 1.3, and 1.7 bar, as determined previously by Castro-Muñoz and Yáñez-Fernández (2015). The authors performed the experiments in batch configuration mode (at 25 °C, Q_f of 58 L/h), that is, recycling the retentate stream and separately collecting the permeate. At each step, the feed stream was coming for the previous membrane step; for example, MF-Permeate was used as the feed for UF100 step, while the UF100-permeate was then the feed for the final UF1 step.

Table 1
Specifications of the membranes employed for the fractionation of Nejayote.

Characteristics	Membrane code		
	MF	UF100	UF1
Model	CFP-1-E−4A	UFP-100-E−4A	UFP-1-E−4
Manufacturer	Amersham Biosciences	Amersham Biosciences	A/G Technology
Membrane type	Microfiltration	Ultrafiltration	Ultrafiltration
MWCO	0.1 μm	100 kDa	1 kDa
Membrane surface area	420 cm^2	420 cm^2	420 cm^2
Membrane material	Polysulfone	Polysulfone	Polysulfone
Configuration	Hollow fiber filter cartridges	Hollow fiber filter cartridges	Hollow fiber filter cartridges

2.3. Membrane permeability

The membrane water permeability (Lp) was determined in all membranes before and after the filtration of Nejayote. The experiments were carried out on total recycling mode using water as feed at 25 °C and Q_f of 58 L/h. The Lp (expressed as kg/m^2 h bar) was determined by Darcy's law, which is denoted as the slope of the straight line obtained plotting the water flux (J_w, kg/m^2 h) at different TMP values, as expressed in Eqs. (4) and (5):

$$J_w = \frac{\dot{m}_p}{A} \tag{4}$$

$$Lp = \frac{J_w}{TMP} \tag{5}$$

where $\dot{m}_p$ (kg/h) refers to the mass flow, A (m^2) refers to the membrane area, and TMP (bar) refers to the applied pressure into the system (Díaz-Montes et al., 2020a). The membrane fouling index (FI, %) was calculated by Eq. (6):

$$FI = \left(1 - \frac{Lp_1}{Lp_0}\right) * 100 \tag{6}$$

where Lp_0 (kg/m^2 h bar) and Lp_1 (kg/m^2 h bar) correspond to the water permeabilities measured before and after processes, respectively (Díaz-Montes et al., 2020a). After each process, the membranes were subjected to enzymatic cleaning (Ultrasil 67, Ecolab) at 1% v/v (50 °C, 180 min). The membrane cleaning efficiency (CE, %) was measured by the flux recovery ratio, as expressed by Eq. (7):

$$CE = \left(\frac{Lp_2}{Lp_0}\right) * 100 \tag{7}$$

where Lp_2 (kg/m^2 h bar) corresponds to the water permeability measured after enzymatic cleaning (Díaz-Montes et al., 2020a).

2.4. Physicochemical analysis

The pH was determined in all samples using a laboratory pH-meter (HI 98107, HANNA), which was previously calibrated with buffer solutions (pH 4 and 7). The total dissolved solids (TDS) were determined using a portable analog refractometer (FG-109, Zhifong) and expressed as degrees Brix (°Bx). The total solids content (TS) (g/L) was determined by drying (90 °C, 12 h). Finally, density (ρ) was calculated as the mass and volume ratio and expressed as grams per liter (g/L) (Díaz-Montes et al., 2018).

2.5. Total carbohydrates content analysis

Total carbohydrates content (TCC) was determined by the phenol-sulfuric method; here, 0.5 mL of diluted sample (1:200), 0.5 mL of phenol reagent (5% w/v) and concentrated sulfuric acid (2.5 mL) were mixed and subsequently measured at 490 nm. The results were expressed as grams of glucose equivalents per liter (g GE/L) using a ten-point standard curve of glucose ranged from 0.016 to 0.162 g/L (Díaz-Montes et al., 2020a).

2.6. Sugar content analysis

The identification and quantification of sugars were determined by high-performance liquid chromatography equipped with infrared detector (HPLC-IR, Varian ProStar 9002) using a resin calcium column (300 mm × 7.8 mm and 9 μm particle size, Aminex HPX-87C). For sample preparation, 500 μL of sample was taken to a final volume of 5 mL with hydrochloric acid. The resulting solution was evaporated in a vacuum oven (85 °C, 10 h), reconstituted with 1 mL of water and then diluted (1:3 in water). The sample was eluted with a flow of 0.6 mL/min at detector temperature of 45 °C and column of 65 °C. The identification was made based on retention times (R_T), while the quantification was carried out using a six-point standard curve of glucose (from 0.01 to 0.06 g/L) and fructose (from 0.001 to 0.006 g/L).

2.7. Total phenols content analysis

The total phenolic content (TPC) was determined using the Folin-Ciocalteu technique; 1 mL of the diluted sample (1:20), 1.8 mL of sodium carbonate (7.5% w/v) and 0.6 mL of Folin-Ciocalteu reagent were completely mixed and measured at 760. The results were expressed as milligrams of gallic acid equivalents per liter (mg GAE/L) using a seven-point standard curve of gallic acid (from 6.23 to 43.60 g/L) (Díaz-Montes et al., 2020a).

2.8. Phenolic acids analysis

The identification of phenolic acids was determined by ultra-high performance liquid chromatography equipped with diode array detector (UHPLC-PDA, Thermo Scientific) using a C18 column (50 mm × 2.1 mm and 1.8 μm particle size, Hypersil 3u). The analysis was performed using a mobile phase composed of A: acetonitrile (20%) and B: water-trifluroacetic acid pH 2 (80%) in isocratic conditions, running time of 9.87 min, flow rate of 104 μL/min, and injection volume of 0.3 μL. The elution from the UHPLC was directly introduced into the mass spectrometry (micrOTOF-Q, Bruker) using electrospray ionization (ESI). The detection was by ESI interface in negative ionization mode, scan range of *m/z* 150–950, set capillary of 2.7 kV, set end plate off-set of −500 V, set collision cell RF of 150.0 Vpp, set nebulizer of 1.0 bar, set dry heater of 200 °C, and set dry gas of 6.0 L/min.

2.9. Statistical analysis

Experiments and analytical methods were performed in triplicate and the results were expressed as the mean ± standard deviation (SD). One-way analysis of variance (ANOVA) and correlation analysis were performed using the Statistical Analysis System (SAS Institute Inc.). Tukey's multiple range tests were used to compare the means. Differences among the means of $p < 0.05$ were considered significant.

3. Results and discussion

3.1. Three-step membrane process

In the first process, the crude Nejayote was filtrated through the MF membrane (1.3 bar, 58 L/h, 25 °C) obtaining two fractions, MF-Permeate and MF-Retentate. The MF-permeate fraction was subjected to the second process, UF100 (1.3 bar, 58 L/h, 25 °C), and the UF100-Permeate and UF100-Retentate fractions were obtained. Finally, the UF100-Permeate fraction was filtered through the UF1 process (1.7 bar, 58 L/h, 25 °C), resulting in the UF1-Permeate and UF1-Retentate fractions. The processes were operated in batch concentration mode and the J_p and the VRF were monitored as a function of operating time, as shown in Fig. 1.

In general, the J_p gradually decreased as a function of time while the VRF increased. Importantly, it can be seen that the MF process (Fig. 1A) exhibited the most drastic decrease of J_p (approx. from 400 up to 121 L/m^2 h) during the first 20 min; the UF 100 process (Fig. 1B) also had its highest J_p decay (approx. from 29 up to 23 L/m^2 h) in the first 20 min and subsequently the decrease was almost linear; while in the UF1 process (Fig. 1C), a constant J_p (approx. 3 L/m^2 h) was observed throughout its execution. It is known that the J_p decrease in a membrane process is influenced by the composition of the feed stream and the fouling phenomenon. This behavior in J_p has also been observed during the treatment and clarification of natural juices (e.g., kiwifruit), especially in UF processes (Cassano et al., 2008).

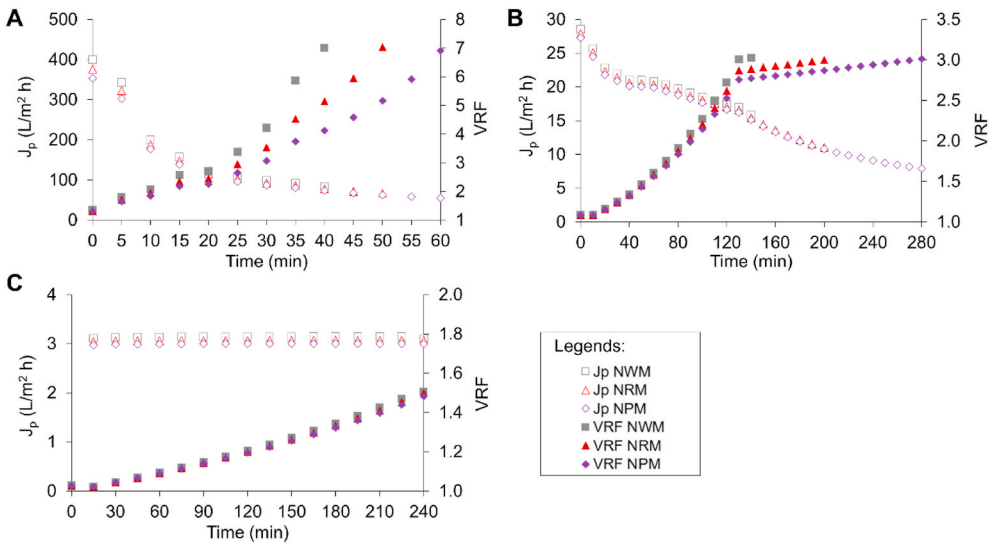

Fig. 1. Volumetric permeate flux (J_p; unfilled markers) and volume reduction factor (VRF; filled markers) of the NWM (gray color), NRM (red color), and NPM (purple color). A) MF (feed: Nejayote; TMP: 1.3 bar; Q_f: 58 L/h; T: 25 °C); UF100 (feed: MF-Permeate; TMP: 1.3 bar; Q_f: 58 L/h; T: 25 °C); UF1 (feed: UF100-Permeate; TMP: 1.7 bar; Q_f: 58 L/h; T: 25 °C). Results expressed with the mean ± SD for each sample ($n = 3$). (For interpretation of the references to color in this figure legend, the reader is referred to the Web version of this article.)

On the other hand, the behavior of the VRF was different in each process and for each type of Nejayote, which was expected according to the different physicochemical composition of the Nejayote. In the MF process (Fig. 1A), VRF gradually increased until a value of 7 when the decrease in J_p had no longer significant changes; however, the filtrated NWM required 40 min to achieve such a value, while the NRM and NPM needed around 50 and 60 min, respectively. The UF100 process (Fig. 1B) reached a VRF value of 3, but each extract (NWM, NRM, and NPM) required different operating time (140, 200 and 240 min, respectively) to achieve it. While in the UF1 process (Fig. 1C) achieved a VRF of 1.5 at 240 min. This difference in operating time was largely due to the composition of the fractions that influenced the fouling of the membrane.

Fig. 2 illustrates the resulting fractions of both retentates and permeates produced during the fractionation of Nejayote (NWM, NRM, and NPM) at each step. A visible change in color tonalities has been observed; for example, the MF-Retentate fractions turned yellow-brown due to the high concentration of carbohydrates; while the UF1-Permeate fractions were translucent, which evidenced the low concentration of carbohydrates but high concentration in phenolic compounds, which will be discussed in detail in further sections.

3.2. Membrane fouling and permeability

In theory, fouling is the deposition of different compounds present in the filtrated extract into the membrane pores; membrane fouling can occur due to cake formation, adsorption blocking, partial or complete blocking (Díaz-Montes and Castro-Muñoz, 2019). Fouling is an inevitable issue in membrane processes and it is dependent on the physicochemical composition of the feed stream (Castro-Muñoz et al., 2016). Therefore, the calculation of the FI is a common practice when characterizing the filtration of any extract. Table 2 enlists the parameters related to the water permeabilities and fouling and cleaning efficiency. The permeability (Lp_0) depends on the MWCO of the membrane (MF > UF100> UF1), however, the fouling depends on the composition of the feed at specific step. For example, the MF membrane presented the

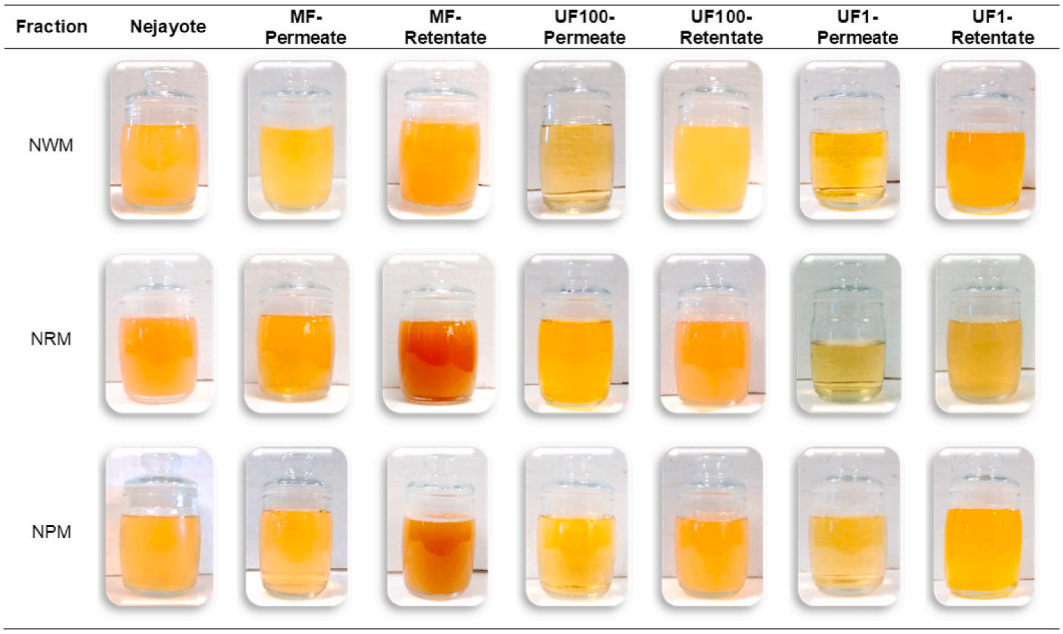

Fig. 2. Physical aspect of the fractions obtained during the fractionation of the NWM, NRM, and NPM using membranes.

Table 2
Water permeability (Lp_0: before process; Lp_1: after process; Lp_2 after cleaning), fouling index (FI), and cleaning efficiency (CE) of MF and UF membranes.

Determination	Membrane code		
	MF	UF100	UF1
Lp_0 (kg/m^2 h bar)	472.75 ± 8.28	248.64 ± 0.00	2.98 ± 0.00
Lp_1 (kg/m^2 h bar)	119.74 ± 1.50	125.31 ± 0.99	1.99 ± 0.00
Lp_2 (kg/m^2 h bar)	412.40 ± 4.70	243.99 ± 4.48	2.59 ± 0.00
FI (%)	74.61 ± 0.71	49.60 ± 0.40	33.33 ± 0.00
CE (%)	87.44 ± 1.77	98.13 ± 1.80	86.96 ± 0.00

Results expressed with the mean ± SD for each sample ($n = 3$).

highest FI value (ca. 74.6%) and the UF1 membrane the lowest FI value (ca. 33.3%), which suggests that the composition of Nejayote was modified thanks to the retention of macromolecules during fractionation. In particular, for the UF1 membrane, some macromolecules with variable size and different shape could be able to clog the pores of the membranes in various ways. It is reported that calcium cations display a bio-flocculation effect in carbohydrates, fats, and proteins (Wan et al., 2020) and thus such agglomerated molecules may cause the obstruction of the membrane (Alazmi et al., 2010). In this way, the carbohydrates from Nejayote probably bio-flocculated due to the presence of calcium hydroxide On the other hand, it has been reported that calcium ions can create a layer of incrustations in UF membranes, causing a permeate flux decrease depending on the ion concentration and the operating time (Prisciandaro et al., 2019). After cleaning protocol, the permeabilities of the membranes (Lp_2) were recovered between 87 and 98% thanks to the enzymatic agent, since its effect is directly on organic material such as polysaccharides (Rudolph et al., 2018).

3.3. Physicochemical composition

The physicochemical composition of Nejayote was determined in terms of pH, TS, TDS, and density (ρ), as shown in Table 3. For the initial extracts, they displayed an extremely alkaline pH (between 12.6 and 13.1), which is directly related to the concentration of calcium hydroxide used within the nixtamalization process. It is known that some fraction (15 and 17%) of the calcium hydroxide is absorbed in the form of calcium by the nixtamalized grain, the remaining is still present in the Nejayote (Ruiz-Gutiérrez et al., 2012; Trejo-Gonzalez et al., 1982). Regarding the TS and TDS, such parameters are the result of the removal of the maize pericarp and the total and partial hydrolysis of the compounds because of the alkaline solution; similarly, such components also influenced the ρ of the resulting wastewater. The physicochemical composition of the resulting indeed depend exclusively on the maize type (Salinas-Moreno et al., 2013).

Even though each type of Nejayote had a different physicochemical composition, however, the variation throughout the integrated membrane system of MF-UF100-UF1 followed the same trend, as detailed in Table 3. Although the pH generated by the addition of calcium hydroxide during the nixtamalization process resulted in a high alkalinity (>12), the pH values progressively decreased compared to the initial extract. In the MF process, the pH decreased between 0.7 and 2.5% depending on the Nejayote type, which was possibly due to the retention of calcium ions in the colloidal mass (e.g., bio-flocculants) that formed on the surface of the membrane (Gul et al., 2021). During the UF100 and UF1 steps, a reduction in pH was noted between 0.8 and 4.4% and between 2.7 and 12.5%, respectively, which could be ascribed to the selectivity of the membrane. In particular, UF membranes have smaller pores than the MF membrane, increasing the rejection of any solute (e.g., calcium) thanks to pore size reduction; furthermore, it was observed that the UF1 membrane had higher rejection compared to that of UF100. In addition to this, it has been reported that in UF membranes the solutes (e.g., calcium chloride, calcium sulphate, tin chloride, and tin sulphate) tend to accumulate due to the polarization effect, which represents an extra barrier for the molecules to pass through (Qadir et al., 2017).

Table 3
Physicochemical composition of NWM, NRM, and NPM, and their fractions obtained after fractionation: pH, density (ρ), total solids (TS), and total dissolved solids (TDS).

Determination	pH	ρ (g/L)	TS (g/L)	TDS (°Bx)
Nejayote				
NWM	12.63 ± 0.01^{c}	893.33 ± 11.55^{b}	0.38 ± 0.01^{b}	1.00 ± 0.00^{b}
NRM	12.83 ± 0.02^{b}	1002.55 ± 1.52^{a}	0.54 ± 0.00^{a}	1.50 ± 0.00^{a}
NPM	13.12 ± 0.04^{a}	998.38 ± 1.95^{b}	0.39 ± 0.01^{b}	1.50 ± 0.00^{a}
MF Process				
NWM				
MF-Permeate	12.41 ± 0.01^{c}	966.67 ± 11.55^{c}	0.27 ± 0.00^{c}	1.20 ± 0.00^{c}
MF-Retentate	12.42 ± 0.01^{c}	980.00 ± 0.00^{bc}	1.72 ± 0.01^{b}	1.10 ± 0.00^{d}
NRM				
MF-Permeate	12.74 ± 0.02^{ab}	995.89 ± 2.77^{a}	0.23 ± 0.02^{c}	1.00 ± 0.00^{e}
MF-Retentate	12.70 ± 0.02^{b}	992.58 ± 1.90^{ab}	2.36 ± 0.17^{a}	2.00 ± 0.00^{b}
NPM				
MF-Permeate	12.79 ± 0.05^{a}	997.51 ± 1.50^{a}	0.25 ± 0.00^{c}	0.50 ± 0.00^{f}
MF-Retentate	12.72 ± 0.05^{b}	1000.09 ± 1.15^{a}	2.54 ± 0.00^{a}	2.50 ± 0.00^{a}
UF100 Process				
NWM				
UF100-Permeate	12.08 ± 0.03^{d}	946.67 ± 11.55^{b}	0.38 ± 0.00^{c}	0.50 ± 0.00^{b}
UF100-Retentate	11.83 ± 0.01^{e}	953.33 ± 11.55^{b}	0.79 ± 0.02^{b}	1.00 ± 0.00^{ab}
NRM				
UF100-Permeate	12.73 ± 0.02^{b}	999.13 ± 1.01^{a}	0.39 ± 0.01^{c}	1.00 ± 0.00^{ab}
UF100-Retentate	12.80 ± 0.01^{a}	991.66 ± 0.55^{a}	0.96 ± 0.00^{a}	1.00 ± 0.00^{b}
NPM				
UF100-Permeate	12.63 ± 0.02^{c}	995.65 ± 3.36^{a}	0.32 ± 0.00^{c}	1.00 ± 0.00^{ab}
UF100-Retentate	12.79 ± 0.01^{a}	983.59 ± 2.19^{a}	0.81 ± 0.09^{b}	1.50 ± 0.00^{a}
UF Process				
NWM				
UF1-Permeate	10.80 ± 0.02^{d}	993.75 ± 0.32^{a}	0.90 ± 0.01^{a}	0.00 ± 0.00^{b}
UF1-Retentate	11.14 ± 0.03^{e}	987.72 ± 0.98^{b}	0.61 ± 0.01^{c}	0.50 ± 0.00^{a}
NRM				
UF1-Permeate	12.48 ± 0.06^{ab}	996.12 ± 2.87^{a}	0.94 ± 0.04^{a}	0.00 ± 0.00^{b}
UF1-Retentate	12.20 ± 0.04^{c}	985.75 ± 1.33^{b}	0.60 ± 0.01^{c}	0.50 ± 0.00^{a}
NPM				
UF1-Permeate	12.52 ± 0.03^{a}	993.20 ± 1.41^{a}	0.82 ± 0.02^{b}	0.00 ± 0.00^{b}
UF1-Retentate	12.38 ± 0.02^{b}	983.43 ± 2.58^{b}	0.48 ± 0.02^{d}	0.50 ± 0.00^{a}

Results expressed with the mean ± SD for each sample ($n = 3$). Different letters in each determination and process indicate a significant difference ($p < 0.05$) according to the Tukey's test.

Over the MF-UF100-UF1 process, the ρ had statistical variation ($p < 0.05$) with values in the range of 946 and 1000 g/L. Interestingly, the decrease in TS and TDS content in each type of Nejayote was more evident (see Table 3); for instance, the MF step retained TDS between 48 and 83%, while the UF100 step retained between 50 and 67%, and the UF1 step retained 100% of the remaining TDS with lower molecular weight. In the case of TS were retained between 1.72 and 2.54 g/L in the

first step, while the second step reached to retain between 0.79 and 0.96 g/L, and finally, the third process exhibited a retention ranged from 0.48 to 0.61 g/L. In general, it was clear that the MF step was good enough to retain the highest content of TS and TDS compared to the other two processes (UF100 and UF1) since the carbohydrates predominate in wastewater and they present larger molecular weight and size. TS includes all dry matter that results from moisture removal; while the TDS include sugars (e.g., mono and disaccharides) and dissolved solids, e.g., flavonoids, phenolics, among others. In any event, most of the retained TS and TDS correspond to the compounds of the maize pericarp, which were hydrolyzed by the alkaline treatment. It is worth mentioning these compounds, including starch, proteins (e.g., albumin, globulin, and zein), fiber (e.g., cellulose and hemicellulose), and lipids (e.g., fatty acids), may present macromolecular sizes (>1 μm) (Hoseney, 1994).

3.4. Recovery of carbohydrates

Carbohydrates are organic molecules composed of carbon, hydrogen, and oxygen, which constitute around 80% of the nutritional value of grains and cereals (e.g., maize, rice, wheat, and barley) in the form of monosaccharides (e.g., glucose and fructose), oligosaccharides (e.g., sucrose and maltose) or polysaccharides (e.g., starch and glycogen) (Hoseney, 1994). The determination of carbohydrates with sulfuric acid method causes an exothermic hydrolysis reaction, breaking down the oligo and polysaccharides in their monosaccharides, which remain dehydrated and reactive with phenol. The monosaccharide-phenol complex is a colored compound that can be quantified by spectrophotometry (BeMiller, 2017).

Maize is constituted in a higher proportion (~70%) by starch, this latter molecule is formed by repeated units of glucose and less proportion (~10%) by cellulose (constituted by repeated units of glucose), hemicellulose (constituted by repeated units of glucose, xylose, arabinose, and galactose), and glucose; in such a way, the percentage of TCC rejection was evaluated by means of the relation between the initial and final content, as shown in Fig. 3A. Initially, the TCC in the NRM (ca. 6.5 g GE/L) was higher with respect to NWM (ca. 2.5 g GE/L) and NPM (ca. 5.1 g GE/L), which is attributed to the chemical composition of the maize. It has been reported that colorful maize contains a higher percentage of carbohydrates (up to 9%) than other varieties (Lavado Soto et al., 2013). Surprisingly, TCC rejection did not follow a specific trend during fractionation. For the MF process, TCC rejection was 19.4, 81.6, and 75.6% (equivalent to 11.6, 16.1, and 19.4 g GE/L, respectively) for NWM, NRM, and NPM, respectively. In the UF100 process, the rejections were 19.6, 39.9 and 11.6%, respectively; while in the UF1 process, the TCC rejection resulted in 39.8, 64.4 and 26.7%, respectively. Parameters influencing component separation via membrane processes are usually temperature, pressure, process time, VRF, membrane characteristics (e.g., material and MWCO) and feed characteristics (e.g., types of solutes) (Mkadmini Hammi et al., 2017). Apart from the evident rejection due to their molecular size, the retention of carbohydrates could be influenced by their nature and kind of membrane, that is, carbohydrates are hydrophilic molecules due to their composition in hydroxyl groups (-OH) (Jorand et al., 1998), which can be rejected by hydrophobic membrane materials, such as polysulfone (Castro-Muñoz, 2019). For instance, Wang and Yu (2021) explained how the membrane pressure causes an increase in the permeate flux due to the compaction and reduction of the membrane thickness, causing an increase in the concentration polarization and eventually a membrane fouling, which could indeed contribute to the rejection of carbohydrates (Cohen et al., 2017). In this study, the filtration processes were carried out consecutively for each type of Nejayote, that is, the NWM was processed through the MF, followed by the NRM and finally the NPM; with rinsing the membrane that entered each process. However, membrane foulants were not completely removed after NWM, which could increase carbohydrate retention of NRM and NPM, as seen in Fig. 3A.

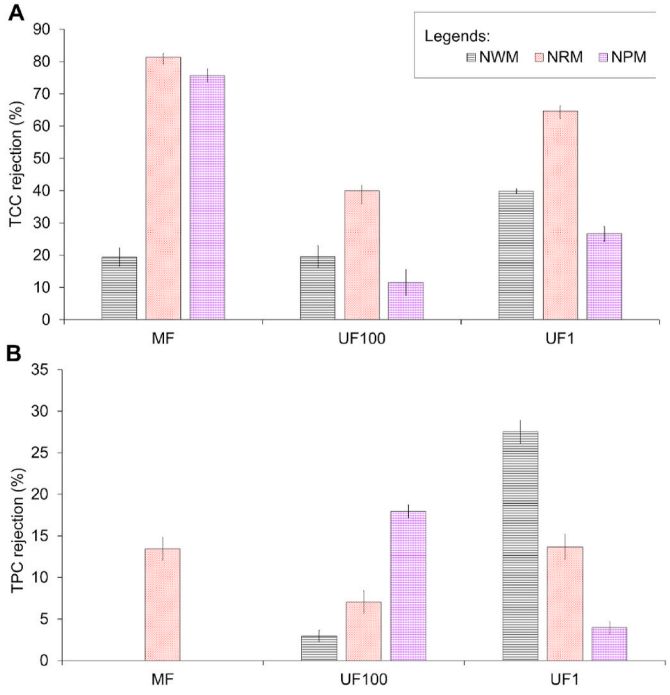

Fig. 3. A) Rejection of total carbohydrates content (TCC) and B) total phenolic content (TPC) during fractionation. Results expressed as the mean ± SD for each sample ($n = 3$).

Castro-Muñoz and Yáñez-Fernández (2015) reported similar TCC retention values than this study when filtrating white corn Nejayote using MF process, however, the retention values during the UF steps (MWCO of 100 and 1 kDa) reported by the authors were higher (~65 and ~75%, respectively) than those determined for NWM with the UF100 and UF1 membranes. Such differences were possibly influenced by the initial carbohydrate concentration and the type of carbohydrates contained in Nejayote, such as simple sugars, fibers, or polysaccharides, which may somehow contribute to membrane fouling (Galanakis, 2015).

3.5. Recovery of phenolic compounds

Phenolic acids (e.g., *p*-hidroxybenzoic, *p*-coumaric, vanillic, and ferulic acids) have been reported in most of varieties of maize (Salinas-Moreno et al., 2017). The determination of phenolic compounds is commonly carried out through redox reactions between the Folin-Ciocalteu reagent (mixture of phosphomolybdic and phosphotungstic acids) and the –OH groups of the aromatic ring, to form a blue complex that can be quantified by spectrophotometry as a function of some specific phenolic compound (Blainski et al., 2013).

Fig. 3B shows the percentage of TPC rejection in each stage after the fractionation process. Initially, the TPC in the NRM and NPM (995 and 915 mg GAE/L, respectively) was twice higher than that of the NWM (429 mg GAE/L). In principle, all membranes cannot retain components with molecular weight lower than their MWCO (1 μm, 100 kDa, and 1 kDa, respectively); however, as previously mentioned, fouling can cause partial or complete pore clogging and thus contribute to the retention of small molecules such as phenolic compounds with molecular weight of ca. 180 g/mol (e.g. hydroxycinnamic acid) (Cassano et al., 2008; Castro-Muñoz and Yáñez-Fernández, 2015). Experimentally, the UF1 step retained approximately 27.5, 13.7 and 3.9% of the phenolic compounds present in the NWM, NRM, and NPM, respectively, which is equivalent to the permeation of 556.8, 691.1, and 746.1 mg GAE/L. At this point, this could be a result of possible interaction between polyethersulfone membrane and polyphenols, along with adsorption fouling. Apart from such evidence, specific interactions, such as hydrophobic and

Coulombic intermolecular, between the molecules and membrane surface (e.g., polyphenols-polyphenols, polyphenols-membrane) can apparently contribute to the polyphenol retention (Crespo and Brazinha, 2010).

On the other hand, there is evidence of the adsorption of phenolic compounds on the membrane surface and inside the pores. Such adsorption is ascribed to polar interactions (e.g., van der Waals) and hydrogen bonds between the –OH groups of phenolic compounds and the membrane; which leads to an increase in their retention (Castro-Muñoz, 2019; Mkadmini Hammi et al., 2017). Arsuaga et al. (2010) explain how the interactions between solutes and the membrane can change the properties of its surface, such as charge and hydrophobicity, which generate new interactions that impair the operation of the process, the performance of filtrations, and increase the probability of irreversible fouling (Arsuaga et al., 2011). In addition, unavoidable interactions are generated between phenolic compounds with macromolecules such as carbohydrates, due to the formation of hydrogen bridges between the –OH groups of phenolic compounds and the oxygens of carbohydrates that are located in the glycosidic bonds (Jakobek, 2015). In such a way, the phenolic components immersed in the polymeric structure and their loss occurs during the rejection of the macromolecules (Castro-Muñoz, 2019).

Despite the phenomena that occurred during the recovery of phenolic compounds, the purpose of using the three-step membrane process was to retain the highest carbohydrate content to obtain a concentrated extract with phenolic acids. Thus, 14 phenolic acids were identified in the final fraction (UF-1 permeate), of which 10 were identified in all types of Nejayote (m/z 377, 377, 193, 163, 237, 329, 207, 311, 311, and 293 $[M-H]^-$), while 3 only in NWM (m/z 539, 385, and 385 $[M-H]^-$), and one in NPM (m/z 939 $[M-H]^-$), as reported in Table 4. The identification of the compounds has been done by analyzing the MS data and some literature reports, as follows:

- *Compound at m/z 163 $[M-H]^-$*: The MS data showed a signal at m/z 162 $[M-H-(15)]^-$ corresponding to the loss of a hydrogen (H^+) and another signal at m/z 119 $[M-H-(44)]^-$ which indicates the carbon dioxide (CO_2) removal. Here, the compound was mainly credited as *p*-coumaric acid (Díaz-Montes et al., 2018).
- *Compound at m/z 193 $[M-H]^-$*: The MS data showed a signal at m/z 178 $[M-H-(15)]^-$, which was due to cleavage of methyl group (CH_3), while a signal at m/z 149 $[M-H-(44)]^-$ could correspond to the removal of CO_2, and the signal at m/z 134 $[M-H-(44+15)]^-$ indicated the removal of CO_2 and CH_3. Therefore, the compound was assigned as ferulic acid (Díaz-Montes et al., 2018).
- *Compound at m/z 207 $[M-H]^-$*: MS data showed a signal at m/z 311 $[M-H+(104)]^-$ which belongs to caffeoyltartaric acid. The signal at m/z 293 $[M-H+(86)]^-$ corresponds to dehydrated caffeoyltartaric acid. The compound was tentatively assigned as a derivative of caffeoyltartaric acid (Chen et al., 2012).
- *Compound at m/z 293 $[M-H]^-$*. MS data showed a signal at m/z 329 $[M-H+(18+18)]^-$ indicating the addition of two molecules of water (H_2O) and another signal at m/z 112 $[M-H-(162+18+1)]^-$ corresponding to hydrated caffeic acid. The compound was tentatively assigned as a derivative of caffeoyltartaric acid (Chen et al., 2012; Schütz et al., 2005).
- *Compound at m/z 237 $[M-H]^-$*: MS data showed signals at m/z 112, 237, and 238 $[M-H]^-$. Particularly, the signal at m/z 112 $[M-H-(125)]^-$ could correspond to the loss of CO_2 and H_2O molecules, however, there is no identification of this phenolic compound so far.
- *Compound at m/z 311 $[M-H]^-$*: MS data showed compounds at different retention time (R_T) with a signal at m/z 293 $[M-H-(18)]^-$, which indicates the elimination of H_2O, while the signal at m/z 208 $[M-H-(44+44+15)]^-$ refers to the elimination of CO_2 and a CH_3 groups. The compounds were tentatively assigned as isomers of caffeoyltartaric acid (Chen et al., 2012; Schütz et al., 2005).

Table 4
Mass spectral data used for identification of phenolic acids in Nejayote from white (NWM), red (NRM), and purple (NPM) maize.

N° of signal	R_T (min)	$[M-H]^-$ (m/z)	MS ions (m/z)	Tentative identify	Reference
NWM					
1	2.4	539	133, 165, 179, 191, **539**, 540, 541, 881, 882, 883	Unknown	–
2	2.5	377	179, **377**, 378, 379, 521, 719, 720, 721, 1061, 1062, 1063	Caffeic acid derivative	Bystrom et al. (2008)
3	2.7	377	179, **377**, 378, 521, 719, 720, 721, 1061, 1063	Caffeic acid derivative	Bystrom et al. (2008)
4	5.9	193	112, 134, 149, 178, **193**, 194	Ferulic acid	Díaz-Montes et al. (2018)
5	6.4	163	112, 119, 162, **163**, 164, 715	*p*-Coumaric acid	Díaz-Montes et al. (2018)
6	6.8	385	112,193, **385**, 386, 713, 714, 715, 716	Dehydrodiferulic acid	Ralph et al. (1994)
7	7.4	385	112, 193, **385**, 386, 713, 714, 715	Dehydrodiferulic acid	Ralph et al. (1994)
8	13.9	237	112, **237**, 238	Unknown	–
9	15	329	112, 293, **329**, 330, 331	Dihydroxyphenyllactoyl-tartaric acid	Chen et al. (2012)
10	16.1	207	112, 115, **207**, 208, 293, 294, 311, 312, 329, 713	Caffeoyltartaric acid derivate	Chen et al. (2012)
11	16.2	311	112, 207, 208, 293, **311**, 312	Caffeoyltartaric acid isomer	(Chen et al., 2012; Schütz et al., 2005)
12	16.8	293	112, **293**, 329	Caffeoyltartaric acid derivate	(Chen et al., 2012; Schütz et al., 2005)
13	18.5	311	112, 115, 237, **311**, 312, 347, 623	Caffeoyltartaric acid isomer	(Chen et al., 2012; Schütz et al., 2005)
NRM					
1	2.5	377	179, **377**, 379, 521, 719, 720, 721, 1061, 1062, 1063	Caffeic acid derivative	Bystrom et al. (2008)
2	2.8	377	179, **377**, 378, 379, 387, 521, 719, 720, 721, 1061	Caffeic acid derivative	Bystrom et al. (2008)
3	5.9	193	134, 149, 178, **193**, 194	Ferulic acid	Díaz-Montes et al. (2018)

(*continued on next page*)

Table 4 (*continued*)

N° of signal	R_T (min)	$[M-H]^-$ (m/z)	MS ions (m/z)	Tentative identify	Reference
4	6.4	163	119, 162, **163**, 164	*p*-Coumaric acid	Díaz-Montes et al. (2018)
5	13.9	237	**237**, 238	Unknown	–
6	15	329	293, **329**, 330, 331	Dihydroxyphenyllactoyl-tartaric acid	Chen et al. (2012)
7	16.1	207	**207**, 293, 311, 312, 329	Caffeoyltartaric acid derivate	Chen et al. (2012)
8	16.2	311	207, 293, **311**, 312	Caffeoyltartaric acid isomer	(Chen et al., 2012; Schütz et al., 2005)
9	16.8	293	112, **293**	Caffeoyltartaric acid derivate	(Chen et al., 2012; Schütz et al., 2005)
10	18.5	311	**311**, 312, 347, 623	Caffeoyltartaric acid isomer	(Chen et al., 2012; Schütz et al., 2005)
NPM					
1	2.5	377	179, 341, **377**, 378, 379, 387, 719, 721, 1061, 1063	Caffeic acid derivative	Bystrom et al. (2008)
2	2.7	377	179, **377**, 378, 379, 387, 521, 719, 720, 721, 1061	Caffeic acid derivative	Bystrom et al. (2008)
3	5.9	193	112, 134, 149, 178, **193**, 194	Ferulic acid	Díaz-Montes et al. (2018)
4	6.4	163	112, 119, 162, **163**, 164	*p*-Coumaric acid	Díaz-Montes et al. (2018)
5	8.2	939	147, 713, **939**, 940, 941, 942	Unknown	–
6	13.9	237	112, **237**, 238	Unknown	–
7	15	329	112, 115, 237, 293, **329**, 330, 331	Dihydroxyphenyllactoyl-tartaric acid	Chen et al. (2012)
8	16.2	207	112, **207**, 208, 293, 294, 311, 312, 329	Caffeoyltartaric acid derivate	Chen et al. (2012)
9	16.2	311	112, 207, 208, 237, 293, 310, **311**, 312	Caffeoyltartaric acid isomer	(Chen et al., 2012; Schütz et al., 2005)
10	16.8	293	115, 237, **293**, 311, 329, 713	Caffeoyltartaric acid derivate	(Chen et al., 2012; Schütz et al., 2005)
11	18.5	311	112, 115, **311**, 312, 313, 347, 623, 713	Caffeoyltartaric acid isomer	(Chen et al., 2012; Schütz et al., 2005)

- *Compound at m/z 329 [M-H]*$^-$: The MS data with signal at m/z 293 [M-H-(18 + 18)]$^-$ indicates the removal of two H_2O molecules. The compound was tentatively assigned as dihydroxyphenyllactoyl-tartaric acid (Chen et al., 2012).
- *Compound at m/z 377 [M-H]*$^-$*:* MS data at different R_T with a signal at m/z 179 [M-H-(198)]$^-$ could correspond to caffeic acid. The rest of the signals are possibly belonging to polymeric compounds of caffeic acid. Both compounds were tentatively assigned as derivatives of caffeic acid (Bystrom et al., 2008).
- *Compound at m/z 385 [M-H]*$^-$. MS data at different R_T with a signal at m/z 193 [M-H-(192)]$^-$ could correspond to ferulic acid. The rest of the signals are possibly belonging to dimers of ferulic acid. Both compounds were tentatively assigned as dehydrodiferulic acid (Ralph et al., 1994).

The general properties of phenolic compounds (e.g., catechin and caffeic acid, and vitamin C) allow their application in different areas, for example, within the food industry, they have been used as food additives since they delay the oxidation of foods with a high content of lipids, protect food with high humidity and water activity against microbial attack (e.g., bacteria and yeast), improve both antioxidant properties and nutritional quality of products (Galanakis, 2018). In the cosmetic industry, specific phenolic compounds (e.g., parabens and benzophenon derivatives) are used as ingredients in sun blockers and creams, because they counteract aging caused by free radicals and UV rays (Galanakis et al., 2018). While, in the medical area, some phenolic compounds are used to treat diseases caused by oxidative stress such as diabetes because they neutralize reactive species, inhibit the enzymes that produce reactive species, and participate in the regulation of glucose and inulin receptors, or cancer (e.g., hydroxybenzoic and hydroxycinnamic acids), by blocking the enzymes responsible for mutagenic activities. In general, the current demand for phenolic compounds increases, especially for phenolic acids (Kumar and Goel, 2019).

4. Conclusions

A three-step membrane process was good enough to fractionate the different types of Nejayote. After the fractionation, the initial membrane water permeabilities were recovered over 80% after treating the alkaline wastewater. When dealing with the extraction of high-added value compounds, the MF step essentially retained most of the carbohydrates. The UF100 and UF1 steps allowed the partial extraction of phenolic compounds, where the UF1 offered high retention to concentrate them. The extracted compounds could be used as ingredients in food products; for example, carbohydrates and simple sugars (i.e., glucose and fructose) in bread or other baked products, and phenolic acids (i.e., ferulic and *p*-coumaric acids, and their derivatives) could enrich any potential functional products. Of course, their application would need additional purification technologies (e.g., nanofiltration). Considering the identification of the main phenolic fractions contained in Nejayote. Regardless of the composition of the Nejayote, this work evidences the potentiality of membranes to recover low molecular weight nutraceuticals from the extract in a simple but effective manner.

CRediT authorship contribution statement

Elsa Díaz-Montes: Conceptualization, Investigation, Formal analysis, Writing – original draft, Writing – review & editing, &, Visualization. **Roberto Castro-Muñoz:** Writing – review & editing, Supervision, Validation, All authors have read and agreed to the published version of the manuscript.

Declaration of competing interest

The authors declare that they have no known competing financial interests or personal relationships that could have appeared to influence the work reported in this paper.

Acknowledgment

E. Díaz-Montes thanks to the Consejo Nacional de Ciencia y Tecnología (CONACyT No. 593731) for the financing granted and the Centro de Nanociencias y Micro y Nanotecnologías of the Instituto Politécnico Nacional (CNMN-IPN) for the collaboration as well as Dra. Elvira Ríos Leal (CINVESTAV) and Dr. Jorge Yáñez Fernández (UPIBI-IPN) for their

contribution to this project. Financial support from Polish National Agency for Academic Exchange (NAWA) under Ulam Programme (Agreement No. PPN/ULM/2020/1/00005/U/00001) is gratefully acknowledged. R. Castro-Muñoz also acknowledges the School of Engineering and Science and the FEMSA-Biotechnology Center at Tecnológico de Monterrey for their support through the Bioprocess (0020209I13) Focus Group.

References

Alazmi, R., Nassehi, V., Wakeman, R., 2010. Calcium cation interactions with polysaccharides and proteins in wastewater UF membrane fouling. Membr. Technol. 6–12. https://doi.org/10.1016/S0958-2118(10)70015-X, 2010.

Arboleda Mejia, J.A., Ricci, A., Figueiredo, A.S., Versari, A., Cassano, A., Parpinello, G.P., de Pinho, M.N., 2020. Recovery of phenolic compounds from red grape pomace extract through nanofiltration membranes. Foods 9. https://doi.org/10.3390/foods9111649.

Arsuaga, J.M., López-Muñoz, M.J., Sotto, A., 2010. Correlation between retention and adsorption of phenolic compounds in nanofiltration membranes. Desalination 250, 829–832. https://doi.org/10.1016/j.desal.2008.11.051.

Arsuaga, J.M., Sotto, A., López-Muñoz, M.J., Braeken, L., 2011. Influence of type and position of functional groups of phenolic compounds on NF/RO performance. J. Membr. Sci. 372, 380–386. https://doi.org/10.1016/j.memsci.2011.02.020.

Bacchetti, T., Masciangelo, S., Micheletti, A., Ferretti, G., 2013. Carotenoids, phenolic compounds and antioxidant capacity of five local Italian corn (Zea mays L.) kernels. J. Nutr. Food Sci. 3, 1000237. https://doi.org/10.4172/2155-9600.1000237.

Bello-Pérez, L.A., Camelo-Mendez, G.A., Agama-Acevedo, E., Utrilla-Coello, R.G., 2016. Nutraceutic aspects of pigmented maize: digestibility of carbohydrates and anthocyanins. Agrociencia 50, 1041–1063.

BeMiller, J.N., 2017. Carbohydrate analysis. In: Nielsen, S. (Ed.), Food Analysis. Springer International Publishing, pp. 333–360. https://doi.org/10.1007/978-3-319-45776-5.

Blainski, A., Lopes, G.C., de Mello, J.C.P., 2013. Application and analysis of the Folin Ciocalteu method for the determination of the total phenolic content from Limonium brasiliense L. Molecules 18, 6852–6865. https://doi.org/10.3390/molecules18066852.

Bursać Kovačević, D., Barba, F.J., Granato, D., Galanakis, C.M., Herceg, Z., Dragović-Uzelac, V., Putnik, P., 2018. Pressurized hot water extraction (PHWE) for the green recovery of bioactive compounds and steviol glycosides from Stevia rebaudiana Bertoni leaves. Food Chem. 254, 150–157. https://doi.org/10.1016/j.foodchem.2018.01.192.

Bystrom, L.M., Lewis, B.A., Brown, D.L., Rodriguez, E., Obendorf, R.L., 2008. Characterisation of phenolics by LC-UV/Vis, LC-MS/MS and sugars by GC in Melicoccus bijugatus Jacq. "Montgomery" fruits. Food Chem. 111, 1017–1024. https://doi.org/10.1016/j.foodchem.2008.04.058.

Cassano, A., Donato, L., Conidi, C., Drioli, E., 2008. Recovery of bioactive compounds in kiwifruit juice by ultrafiltration. Innovat. Food Sci. Emerg. Technol. 9, 556–562. https://doi.org/10.1016/j.ifset.2008.03.004.

Castro-Muñoz, R., 2019. Retention profile on the physicochemical properties of maize cooking by-product using a tight ultrafiltration membrane. Chem. Eng. Commun. 1–9. https://doi.org/10.1080/00986445.2019.1618844.

Castro-Muñoz, R., Barragán-Huerta, B.E., Yáñez-Fernández, J., 2016. The use of nixtamalization waste waters clarified by ultrafiltration for production of a fraction rich in phenolic compounds. Waste and Biomass Valorization 7, 1167–1176. https://doi.org/10.1007/s12649-016-9512-6.

Castro-Muñoz, R., García-Depraect, O., León-Becerril, E., Cassano, A., Conidi, C., Fíla, V., 2021. Recovery of protein-based compounds from meat by-products by membrane-assisted separations: a review. J. Chem. Technol. Biotechnol. 96, 3025–3042. https://doi.org/10.1002/jctb.6824.

Castro-Muñoz, R., Yañez-Fernandez, J., 2015. Valorization of Nixtamalization wastewaters (Nejayote) by integrated membrane process. Food Bioprod. Process. 95 https://doi.org/10.1016/j.fbp.2015.03.006.

Castro-Muñoz, R., Yáñez-Fernández, J., 2015. Valorization of Nixtamalization wastewaters (Nejayote) by integrated membrane process. Food Bioprod. Process. 95, 7–18. https://doi.org/10.1016/j.fbp.2015.03.006.

Chen, H., Zhang, H., Tian, J., Shi, J., Linhardt, R.J., Ye, T.D.X., Chen, S., 2019. Recovery of high value-added nutrients from fruit and vegetable industrial wastewater. Compr. Rev. Food Sci. Food Saf. 18, 1388–1402. https://doi.org/10.1111/1541-4337.12477.

Chen, H.J., Inbaraj, B.S., Chen, B.H., 2012. Determination of phenolic acids and flavonoids in Taraxacum formosanum kitam by liquid chromatography-tandem mass spectrometry coupled with a post-column derivatization technique. Int. J. Mol. Sci. 13, 260–285. https://doi.org/10.3390/ijms13010260.

Cohen, J.L., Barile, D., Liu, Y., de Moura Bell, J.M.L.N., 2017. Role of pH in the recovery of bovine milk oligosaccharides from colostrum whey permeate by nanofiltration. Int. Dairy J. 66, 68–75. https://doi.org/10.1016/j.idairyj.2016.10.016.

Conidi, C., Castro-Muñoz, R., Cassano, A., 2020. Membrane-based operations in the fruit juice processing industry: a review. Beverages 6, 1–39. https://doi.org/10.3390/beverages6010018.

Crespo, J.G., Brazinha, C., 2010. Membrane processing: natural antioxidants from winemaking by-products. Filtr. Sep. 47, 32–35. https://doi.org/10.1016/S0015-1882(10)70079-3.

Deng, Q., Zinoviadou, K.G., Galanakis, C.M., Orlien, V., Grimi, N., Vorobiev, E., Lebovka, N., Barba, F.J., 2015. The effects of conventional and non-conventional processing on glucosinolates and its derived forms, isothiocyanates: extraction, degradation, and applications. Food Eng. Rev. 7, 357–381. https://doi.org/10.1007/s12393-014-9104-9.

Díaz-Montes, E., Barragán-Huerta, B.E., Yáñez-Fernández, J., 2018. Identification and evaluation of antioxidant activity of hydroxycinnamic acids extracted by ultrafiltration from three varieties of Mexican maize. Waste Biomass Valorization. https://doi.org/10.1007/s12649-018-0420-9.

Díaz-Montes, E., Castro-Muñoz, R., 2019. Metabolites recovery from fermentation broths via pressure-driven membrane processes. Asia Pac. J. Chem. Eng. e2332, 22. https://doi.org/10.1002/apj.2332.

Díaz-Montes, E., Castro-Muñoz, R., Yáñez-Fernández, J., 2016. An overview of nejayote, a nixtamalization by product. Ing. Agrícola y Biosist. 8, 41–60. https://doi.org/10.5154/r.inagbi.2016.03.002.

Díaz-Montes, E., García-Depraect, O., Castro-Muñoz, R., 2021. Membrane technologies for the extraction and purification of steviol glycosides. In: Galanakis, C.M. (Ed.), Steviol Glycosides: Production, Properties, and Applications. Academic Press, Inc., pp. 159–199

Díaz-Montes, E., Gutiérrez-Macías, P., Orozco-Álvarez, C., Castro-Muñoz, R., 2020a. Fractionation of Stevia rebaudiana aqueous extracts via two-step ultrafiltration process: towards rebaudioside a extraction. Food Bioprod. Process. 123, 111–122. https://doi.org/10.1016/j.fbp.2020.06.010.

Díaz-Montes, E., Yáñez-Fernández, J., Castro-Muñoz, R., 2020b. Microfiltration-mediated extraction of dextran produced by Leuconostoc mesenteroides SF3. Food Bioprod. Process. 119, 317–328. https://doi.org/10.1016/j.fbp.2019.11.017.

Galanakis, C.M., 2021. Functionality of food components and emerging technologies. Foods 10, 128. https://doi.org/10.3390/foods10010128.

Galanakis, C.M., 2020. The food systems in the era of the coronavirus (COVID-19) pandemic crisis. Foods 9, 523. https://doi.org/10.3390/foods9040523.

Galanakis, C.M., 2018. Phenols recovered from olive mill wastewater as additives in meat products. Trends Food Sci. Technol. 79, 98–105. https://doi.org/10.1016/j.tifs.2018.07.010.

Galanakis, C.M., 2015. Separation of functional macromolecules and micromolecules: from ultrafiltration to the border of nanofiltration. Trends Food Sci. Technol. 42, 44–63. https://doi.org/10.1016/j.tifs.2014.11.005.

Galanakis, C.M., 2012. Recovery of high added-value components from food wastes: conventional, emerging technologies and commercialized applications. Trends Food Sci. Technol. 26, 68–87. https://doi.org/10.1016/j.tifs.2012.03.003.

Galanakis, C.M., Aldawoud, T.M.S., Rizou, M., Rowan, N.J., Ibrahim, S.A., 2020. Food ingredients and active compounds against the coronavirus disease (COVID-19) pandemic: a comprehensive review. Foods 9, 1701.

Galanakis, C.M., Castro-Muñoz, R., Cassano, A., Conidi, C., 2016. Recovery of High-Added-Value Compounds from Food Waste by Membrane Technology, Membrane Technologies for Biorefining. https://doi.org/10.1016/B978-0-08-100451-7.00008-6.

Galanakis, C.M., Rizou, M., Aldawoud, T.M.S., Ucak, I., Rowan, N.J., 2021. Innovations and technology disruptions in the food sector within the COVID-19 pandemic and post-lockdown era. Trends Food Sci. Technol. 110, 193–200. https://doi.org/10.1016/j.tifs.2021.02.002.

Galanakis, C.M., Tsatalas, P., Galanakis, I.M., 2018. Implementation of phenols recovered from olive mill wastewater as UV booster in cosmetics. Ind. Crop. Prod. 111, 30–37. https://doi.org/10.1016/j.indcrop.2017.09.058.

Gul, A., Hruza, J., Yalcinkaya, F., 2021. Fouling and chemical cleaning of microfiltration membranes: a mini-review. Polymers 13, 846. https://doi.org/10.3390/polym13060846.

Gutiérrez-Uribe, J.A., Rojas-García, C., García-Lara, S., Serna-Saldivar, S.O., 2010. Phytochemical analysis of wastewater (nejayote) obtained after lime-cooking of different types of maize kernels processed into masa for tortillas. J. Cereal. Sci. 52, 410–416. https://doi.org/10.1016/j.jcs.2010.07.003.

Hernández-Martínez, V., Salinas-Moreno, Y., Ramírez-Díaz, J.L., Vázquez-Carrillo, G., Domínguez-López, A., Ramírez-Romero, A.G., 2016. Color, phenolic composition and antioxidant activity of blue tortillas from Mexican maize races. CYTA - J. Food 14, 473–481. https://doi.org/10.1080/19476337.2015.1136842.

Hoseney, R.C., 1994. Principles of Cereal Science and Technology, second ed. American Association of Cereal Chemists, Inc.

Jakobek, L., 2015. Interactions of polyphenols with carbohydrates, lipids and proteins. Food Chem. 175, 556–567. https://doi.org/10.1016/j.foodchem.2014.12.013.

Jorand, F., Boué-Bigne, F., Block, J.C., Urbain, V., 1998. Hydrophobic/hydrophilic properties of activated sludge exopolymeric substances. Water Sci. Technol. 37, 307–315. https://doi.org/10.1016/S0273-1223(98)00123-1.

Kumar, N., Goel, N., 2019. Phenolic acids: natural versatile molecules with promising therapeutic applications. Biotechnol. Rep. 24, e00370 https://doi.org/10.1016/j.btre.2019.e00370.

Lavado Soto, M.A., Raez Guevara, L., Robles Calderon, R., 2013. El maíz morado como materia prima industrial. Rev. la Fac. Ing. Ind. 15, 85–91. https://doi.org/10.15381/idata.v16i1.6422.

Méndez-Lagunas, L.L., Cruz-Gracida, M., Barriada-Bernal, L.G., Rodríguez-Méndez, L.I., 2020. Profile of phenolic acids, antioxidant activity and total phenolic compounds during blue corn tortilla processing and its bioaccessibility. J. Food Sci. Technol. 57, 4688–4696. https://doi.org/10.1007/s13197-020-04505-3.

Mkadmini Hammi, K., Jellouli Ennigrou, D., Majdoub, H., Ksouri, R., 2017. Recovery of phenolic compounds and carbohydrates from hydro-ethanolic extract of Zizyphus lotus fruit using ultrafiltration process. Int. J. Food Eng. 13, 1–13. https://doi.org/10.1515/ijfe-2017-0343.

Nagarajan, J., Heng, W.W., Galanakis, C.M., Ramanan, R.N., Raghunandan, M.E., Sun, J., Ismail, A., Beng-Ti, T., Prasad, K.N., 2016. Extraction of phytochemicals using hydrotropic solvents. Separ. Sci. Technol. 51, 1151–1165. https://doi.org/10.1080/01496395.2016.1143842.

Niño-Medina, G., Carvajal-Millán, E., Lizardi, J., Rascon-Chu, A., Marquez-Escalante, J. A., Gardea, A., Martinez-Lopez, A.L., Guerrero, V., 2009. Maize processing waste water arabinoxylans: gelling capability and cross-linking content. Food Chem. 115, 1286–1290. https://doi.org/10.1016/j.foodchem.2009.01.046.

Prisciandaro, M., Innocenzi, V., Tortora, F., di Celso, G.M., 2019. Reduction of fouling and scaling by calcium ions on an UF membrane surface for an enhanced water pre-treatment. Water 11, 1–11. https://doi.org/10.3390/w11050984.

Prochaska, K., Antczak, J., Szczygie, M., 2018. Removal of succinic acid from fermentation broth by multistage process (membrane separation and reactive extraction). Separ. Purif. Technol. 192, 360–368. https://doi.org/10.1016/j.seppur.2017.10.043.

Qadir, D., Mukhtar, H.B., Keong, L.K., 2017. Rejection of divalent ions in commercial tubular membranes: effect of feed concentration and anion type. Sustain. Environ. Res. 27, 103–106. https://doi.org/10.1016/j.serj.2016.12.002.

Ralph, J., Quideau, S., Grabber, J.H., Hatfield, R.D., 1994. Identification and synthesis of new ferulic acid dehydrodimers present in grass cell walls. J. Chem. Soc. Perkin Trans. 1 602, 3485–3498. https://doi.org/10.1039/p19940003485.

Rudolph, G., Schagerlöf, H., Krogh, K.B.M., Jönsson, A., Lipnizki, F., 2018. Investigations of Alkaline and Enzymatic Membrane Cleaning of Ultrafiltration Membranes Fouled by Thermomechanical Pulping Process Water. https://doi.org/10.3390/membranes8040091.

Ruiz-Gutiérrez, M.G., Quintero-Ramos, A., Meléndez-Pizarro, C.O., Talamás-Abbud, R., Barnard, J., Márquez-Meléndez, R., Lardizábal-Gutiérrez, D., 2012. Nixtamalization in two steps with different calcium salts and the relationship with chemical, texture and thermal properties in masa and tortilla. J. Food Process. Eng. 35, 772–783. https://doi.org/10.1111/j.1745-4530.2010.00627.x.

Salinas-Moreno, Y., Aragón Cuevas, F., Ybarra Moncada, C., Aguilar Villarreal, J., Altunar López, B., Sosa Montes, E., 2013. Caracterización física y composición química de razas de maíz de grano azul/morado de las regiones tropicales y subtropicales de Oaxaca. Rev. Fitotec. Mex. 36, 23–31. https://doi.org/10.35196/rfm.2013.1.23.

Salinas-Moreno, Y., García-Salinas, C., Ramírez-Díaz, J.L., Alemán-de la Torre, I., 2017. Phenolic compounds in maize grains and its nixtamalized products. In: Soto-Hernández, M. (Ed.), Phenolic Compounds - Natural Sources, Importance and Applications, pp. 215–232. https://doi.org/10.5772/66893. IntechOpen.

Sarfarazi, M., Jafari, S.M., Rajabzadeh, G., Galanakis, C.M., 2020. Evaluation of microwave-assisted extraction technology for separation of bioactive components of saffron (Crocus sativus L.). Ind. Crop. Prod. 145, 111978. https://doi.org/10.1016/j.indcrop.2019.111978.

Schütz, K., Kammerer, D.R., Carle, R., Schieber, A., 2005. Characterization of phenolic acids and flavonoids in dandelion (Taraxacum officinale WEB. ex WIGG.) root and herb by high-performance liquid chromatography/electrospray ionization mass spectrometry. Rapid Commun. Mass Spectrom. 19, 179–186. https://doi.org/10.1002/rcm.1767.

Serna-Saldivar, S.O., Rooney, L.W., 2015. Industrial production of maize tortillas and snacks. In: Rooney, L.W., Serna-Saldivar, S.O. (Eds.), Tortillas: Wheat Flour and Corn Products. AACC International, Inc., Minnesota , U.S.A., pp. 247–281. https://doi.org/10.1016/B978-1-891127-88-5.50013-X

Syedd-León, R., Orozco, R., Álvarez, V., Carvajal, Y., Rodríguez, G., 2020. Chemical and antioxidant charaterization of native corn germplasm from two regions of Costa Rica: a conservation approach. Int. J. Food Sci. https://doi.org/10.1155/2020/2439541, 2020.

Trejo-Gonzalez, A., Feria-Morales, A., Wild-Altamirano, C., 1982. The role of lime in the alkaline treatment of corn for tortilla preparation. In: Feeney, R.E., Whitaker, J.R. (Eds.), Modification of Proteins Food, Nutritional, and Pharmacological Aspects. American Chemical Society, pp. 245–263. https://doi.org/10.1021/ba-1982-0198.ch009.

Valderrama-Bravo, C., López-Ramírez, Y., Jiménez-Ambriz, S., Oaxaca-Luna, A., Domínguez-Pacheco, A., Hernández-Aguilar, C., Moreno-Martínez, E., 2015. Changes in chemical, viscoelastic, and textural properties of nixtamalized dough with nejayote. LWT - Food Sci. Technol. (Lebensmittel-Wissenschaft -Technol.) 61, 496–502. https://doi.org/10.1016/j.lwt.2014.12.038.

Velasco-Martinez, M., Angulo, O., Vazquez-Couturier, D.L., Arroyo-Lara, A., Monroy-Rivera, J.A., 1997. Effect of dried solids of nejayote on broiler growth. Poultry Sci. 76, 1531–1534. https://doi.org/10.1093/ps/76.11.1531.

Wan, L., Xiong, L., Zhang, L., Lu, W., 2020. High loaded bioflocculation membrane reactor of novel structure for organic matter recovery from sewage: effect of temperature on bioflocculation and membrane fouling. Water 12, 2497. https://doi.org/10.3390/w12092497.

Wang, Y., Yu, J., 2021. Membrane separation processes for enrichment of bovine and caprine milk oligosaccharides from dairy byproducts. Compr. Rev. Food Sci. Food Saf. 20, 3667–3689. https://doi.org/10.1111/1541-4337.12758.